Ab Initio Modeling of Amide I Coupling in Antiparallel β-Sheets and the Effect of ^{13}C Isotopic Labeling on Infrared Spectra

Petr Bouř*,† and Timothy A. Keiderling*,‡

Institute of Organic Chemistry and Biochemistry, Academy of Sciences of the Czech Republic, Flemingovo nám. 2, 16610, Praha 6, Czech Republic, and Department of Chemistry, University of Illinois at Chicago, 845 West Taylor Street (M/C 111), Chicago, Illinois 60607-7061

Received: November 22, 2004; In Final Form: December 23, 2004

Isotopic substitution with ^{13}C on the amide C═O has become an important means of determining localized structural information about peptide conformations with vibrational spectroscopy. Various approaches to the modeling of the interactions between labeled amide sites, specifically for antiparallel two-stranded, β-forming peptides, were investigated, including different force fields [dipole−dipole interaction vs density functional theory (DFT) treatments], basis sets, and sizes of model peptides used for ab initio calculations, as well as employing models of solvation. For these β-sheet systems the effect of the relative positions of the ^{13}C isotopic labels in each strand on their infrared spectra was investigated. The results suggest that the interaction between labeled amide groups in different strands can be used as an indicator of local β-structure formation, because coupling between close-lying C═O groups on opposing chains leads to the largest frequency shifts, yet some alternate placements can lead to intensity enhancements. The basic character of the coupling interaction between labeled modes on opposing strands is independent of changes in peptide length, water solvent environment, twisting of the sheet structure, and basis set used in the calculations, although the absolute frequencies and detailed coupling magnitudes change under each of these perturbations. In particular, two strands of three amides each contain the basic interactions needed to simulate larger sheets, with the only exception that the C═O groups forming H-bonded rings at the termini can yield different coupling values than central ones of the same structure. Spectral frequencies and intensities were modeled ab initio by DFT primarily at the BPW91/6-31G** level for pairs of three, four, and six amide strands. Comparison to predictions of a classical coupled oscillator model show qualitative but not quantitative agreement with these DFT results.

Introduction

Vibrational spectra, IR and Raman, have long been used to determine average secondary structure characteristics in peptides and proteins.[1−4] Like electronic circular dichroic (ECD) structural studies, the limited resolution of vibrational spectra normally provides sequence-averaged structural information in comparison to the localized details derivable from NMR and X-ray diffraction. Since optical spectra can provide inherently fast measures of structure and are generally applicable to all protein and peptide systems, increasing their information content is of wide interest. Vibrational spectra, in contrast to electronic spectra, have distinctive frequency shifts due to isotopic variation, which can be used to give site-specific characteristics to certain bands for selectively labeled peptides. In the past decade a number of studies have appeared where isotopic substitution was used to obtain better structural insight with IR spectra.[5−21]

Isotopic labeling of the amide group has an important impact on vibrational spectra, because it causes a shift of absorption frequencies and thus allows separation of transitions associated with the labeled residue from those of the rest of the molecule. Thus the properties of this transition reflect the local stereochemistry of the labeled group and its environment. For IR absorption spectra of peptides and proteins, the amide I mode, primarily C═O stretch, has been the dominant diagnostic band used for structural studies. ^{13}C labeling of the C═O in the amide linkage shifts its frequency down by ~40 cm^{-1}, usually resolving the contribution of such labeled residues from the rest of the ^{12}C amide I envelope. Such markers can be straightforwardly incorporated into peptides by substituting commercially available amino acids containing stable isotopes into normal solid-state synthesis procedures.[22] Even greater frequency shifts can be achieved with $^{13}C═^{18}O$ labeling;[23,24] this, however, would increase the material cost significantly. Studies of protein−protein interactions have also been proposed by use of uniform labeling for one member of an interacting system so that the changes in each protein/peptide could be monitored separately.[25−27]

We have previously studied infrared absorption (IR) and vibrational circular dichroism (VCD) of a series of α-helical peptides to determine localized sites of unfolding and the degree of coupling between various sites in the sequence[9,14] and have modeled these with quantum mechanically determined spectral parameters computed for smaller oligomers with constrained (ϕ, ψ) angles and transferred onto larger peptides with the same conformation.[28−30] The degree of coupling between amide groups is the essential physical interaction that makes amide vibrational spectra capable of determining conformation for a polymeric system. Coupling parameters are central to interpretation of data used in recently proposed structural techniques that

* To whom correspondence should be addressed: e-mail bour@uochb.cas.cz,tak@uic.edu.

† Academy of Sciences of the Czech Republic.

‡ University of Illinois at Chicago.

10.1021/jp0446837 CCC: $30.25
Published on Web 02/23/2005

combine Raman polarization and IR data (even including VCD)[31−33] and are vital for the new 2D IR studies that both measure coupling and develop dynamic pictures of protein structure.[34−40] In a recent example, isotopic substitution of helical peptides was used to help determine site-specific coupling.[23] Helices and their interresidue interactions are now fairly well understood, but similar questions with β-sheets are more difficult to resolve, due to their greater heterogeneity and multistranded nature, and they provide natural targets for applications of isotopic labels and their coupling.

A method of growing interest for studying β-sheet formation is to make sequences that form stable β-hairpins.[41−44] Since the turn in the hairpin can be designed synthetically, these monomer forms allow one to place labels in specific positions in the β-sheet part of the molecule, while avoiding complications due to aggregation and interhairpin interactions. Interactions between various sites can be monitored by the spectral response that develops. This paper will focus on simulating vibrational spectra for model two-stranded β-structures, which reflect the conformation of the strands in hairpins, by use of established theoretical methods to systematically investigate the impact of possible coupling patterns between labeled C═O groups. These results provide a basis for interpretation of previous experiments as well as suggest convenient labeling schemes for design of model β-sheet peptides. Our initial studies of unlabeled hairpins stabilized by D-Pro-Gly-based turn sequences[45,46] or by hydrophobic collapse of tryptophan (Trp) residues[47] showed the spectra of the unlabeled sequence to be complex but capable of being qualitatively simulated by theory. Recently we have prepared and successfully theoretically modeled labeled β-hairpins that have differentiable intensity patterns dependent on the type of coupling between the cross-strand labels.[48] All these results suggest the possibility of using isotopic substitution for structural studies on a broader variety of model systems.

Background

Our computational methods for peptide spectral simulations have emphasized use of ab initio quantum mechanical methods to obtain both force fields (FF) and spectral intensities.[29] For large peptide simulations, we have transferred these results from fragments to the larger molecules.[28−30] The basic principle behind this method is to use the best practical theoretical level to calculate the strongest interactions, those between neighboring and near-neighboring residues, which are connected through the polymeric chain or by hydrogen bonding. However, vibrational spectra have traditionally been simulated with empirical FF, and some recent studies of isotopically labeled peptides have taken a simpler approach, focusing on the coupling between oscillators. Electric dipoles and coupling parameters in these models are often determined empirically or with the aid of ab initio computation on very simple systems.[49,50,68,69] These couplings are intrinsic to the ab initio approach as well, but the reduction to the oscillator model can provide a simplified physical model to aid understanding of the coupling phenomenon.

Any two C═O chromophores interact and can be approximately modeled classically by two coupled oscillators (CO) with isolated (monomer) frequencies, ω_1 and ω_2, and vibrational transition dipole moments, μ_1 and μ_2.[20] If isolated, the system of the two oscillators vibrates with new coupled frequencies of

$$\omega_{\pm} = [\omega_1 + \omega_2 \pm \sqrt{(\omega_1 - \omega_2)^2 + 4V^2}]/2$$

where V is a coupling interaction energy,[51] which has been often modeled as a simple dipole−dipole interaction for the vibrational dipole moments (then termed transition dipole coupling, TDC) but is not limited to that. In the case of identical oscillators, $\omega_1 = \omega_2$, the interaction V causes an energy splitting of $2V$ between the two coupled (symmetric and asymmetric, ω_+ and ω_-, respectively) vibrational modes, and results in a significant redistribution of spectral intensity. In real systems, ω_1 and ω_2, even for chemically identical chromophores, are often only approximately equal, because of the influence of the environment. Indeed, this CO method has proven insufficient for vibrational analysis of close-lying, strongly interacting bonds and inferior to full ab initio prediction of the coupling based on a complete molecular harmonic force field, especially for detailed simulation of amide I splittings, isotopic substituent intensities, amide I−II interactions, and VCD band shapes.[10,28,52,70] Thus, even when the CO methodology can provide a good qualitative description of chromophore interactions for special cases,[53,79] more accurate a priori benchmark calculations are needed for definite validation.

The importance of understanding this interaction is enhanced by isotopic substitution, as the labeled bands separate from those of unlabeled groups and split primarily due to their relative coupling, providing a unique focus for analysis. While the ratio of stretching frequencies for unlabeled (ω_{12C}) and labeled (ω_{13C}) species would be inversely proportional to the square root of reduced mass for a diatomic molecule, for the amide I in an isolated amide group, this ratio is computed to be slightly higher ($\sim$1.026, corresponding to a shift of $\sim$43 cm^{-1}) because the C═O stretch mixes with other motions. In peptides, with multiple amide groups, complex coupling patterns may arise, making the normal modes vary from this simple model, but ^{13}C labeling does serve to isolate the local modes of the labeled residues to a significant extent.[14] The value of this simple prediction is reflected in that the experimental differences seen between unlabeled ($\omega_{12C} \sim 1650$ cm^{-1}) and labeled ($\omega_{13C} \sim 1610$ cm^{-1}) amide I modes are clearly detectable. The corresponding weakness is evidenced by the smaller variances that are found with different substitution patterns and structures, as will be discussed in this work.

Calculations

Ab Initio Models. The initial models used for the antiparallel β-sheet structures were based on averaged (idealized) torsion angles, $\{\varphi, \psi, \omega\} = \{-138°, 135°, 180°\}$.[54] An overview of the geometries and calculational methods used can be found in Table 1 and Figure 1. All these structures have two hydrogen-bonded strands but vary in length and presence of solvent, either by including explicit waters or an effective field.[55] In addition, a set of pairs of twisted four-amide strands, with structures taken from our previous paper,[56] were used to test the impact of twist on coupling.

To obtain a sensible force field for higher-frequency modes without a large number of imaginary force constants, the bond lengths and angles of these structures were relaxed by quantum mechanical energy minimization, while the torsion angles were constrained either directly (for structures a and b) or via the normal mode optimization method (for structure c).[57] Density functional theory (DFT) computations at the BPW91/6-31G** level were chosen as the primary method for FF determination because the BPW91 functional[58,59] with this basis set provides good vibrational frequencies with reasonable computational cost for the amide modes of prime interest.[60] Hybrid functionals, often chosen for vibrational spectral studies, do not improve the amide I and II frequencies, which are of interest here, yet lead to much longer computational times, limiting the size of

TABLE 1: Main Structures and Computational Levels Used for the Modeling

structure	(ϕ, ψ)	NS[a]	NA[b]	computational level
2 × 3, Figure 1a	(−139°, 135°)	2	3	HF/6-31G**
				BPW91/6-31G
				BPW91/6-31G*
				BPW91/6-31G**
				BPW91/6-31G**
				BPW91/6-31++G**
2 × 3, Figure 1b	(−139°, 135°)	2	3	BPW91/6-31G** (explicit waters)
2 × 6, Figure 1c	(−137° → −140°, 133° → 136°)[c]	2	6	BPW91/6-31G**
2 × 13, Figure 1d	(−139°, 135°)	2	13	transfer from Figure 1a,c structures
2 × 13, Figure 1e	(−139°, 135°)	2	13	transfer from Figure 1b structure (explicit waters)

[a] NS, number of strands. [b] NA, number of amide groups in each strand. [c] Variation in (ϕ, ψ) due to normal mode minimization of 2 × 6.

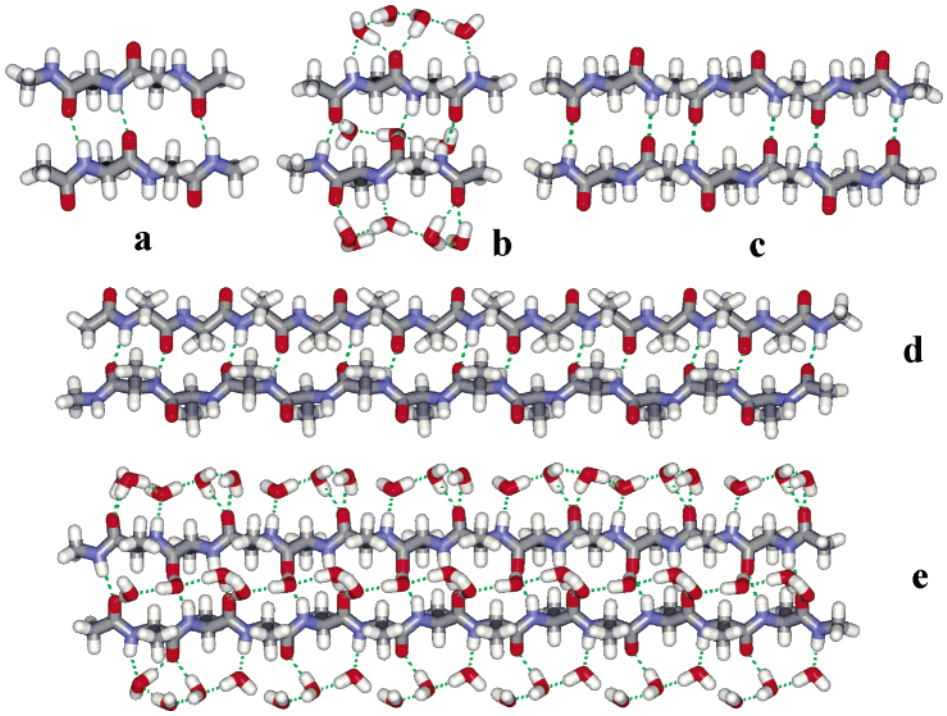

Figure 1. Model antiparallel planar two-stranded β-sheets for spectral simulations; all the peptides fit the formula (Ac-Ala$_n$-NHCH$_3$)$_2$, where n + 1 is the number of amides in a strand. (a) Two triamide strands (2 × 3); (b) two triamide strands plus 12 waters of hydration (2 × 3·12H$_2$O); (c) two hexaamide strands (2 × 6); (d) two 13-amide β-strands (2 × 13); (e) two 13-amide β-strands plus waters of hydration (2 × 13·H$_2$O). Twisted models (2 × 4) were taken from a previous study (see Figure 7).[56]

peptide we can consider at the ab initio DFT level. The Gaussian set of programs[61] was used for all ab initio computations. Force fields and intensity parameters for larger β-sheets were obtained by our Cartesian tensor transfer method[29] by transferring parameters from the ab initio results for the smaller fragments described above to the longer peptides of interest (see Table 1). It might be noted that Choi and Cho[62] have independently developed a somewhat hybrid approach where ab initio-calculated spectral parameters for single residues are transferred onto peptides of various structures. This is a distinctly different approximation from our transfer method using model oligopeptides, in that our method computes local interactions and couplings at an ab initio (DFT) level before transfer.

Unless explicitly noted otherwise, spectra presented here were simulated for the N-deuterated peptides, which corresponds to the way they are normally measured in aqueous solution.[1,6,9,28] Deuteration of solvent additionally removes the coupling and spectral overlap of water vibrations with the amide I mode by shifting the water bending absorption maximum from ∼1640 cm^{-1} (for H$_2$O) to ∼1195 cm^{-1} (for D$_2$O).[28,63,64]

Empirical Modeling. Various TDC models have been used for description of vibrational properties of peptides (and generally polymers with weakly interacting chromophores).[8,20,52,65−69] We tested the performance of this approach in comparison with the ab initio results. For these TDC calculations, the size of the monomer dipole moment was set to 0.48 D to correspond with the average ab initio values. An unperturbed transition frequency of 1650 cm^{-1} was used. The dipole−dipole interaction term was calculated by use of the vacuum permittivity (ϵ_r = 1). As recommended previously,[20] the dipole moment for the ^{13}C═O stretching vibration was placed on the carbonyl carbon, so that the vector deviated by 20° from the C═O bond toward the C$_\alpha$ atom.

Results

Model Testing. To determine the best approach to modeling β-sheet structures, we have investigated the effect of various fragment sizes and different calculational levels. In addition we studied the effects of solvation on the spectral response.

Our initial studies of paired β-strands[10,70,71] used ab initio calculations for (Ac-Ala$_2$-NHCH$_3$)$_2$, each strand containing three amide groups, the minimum number that allows computation of the coupling between terminal and central amides and

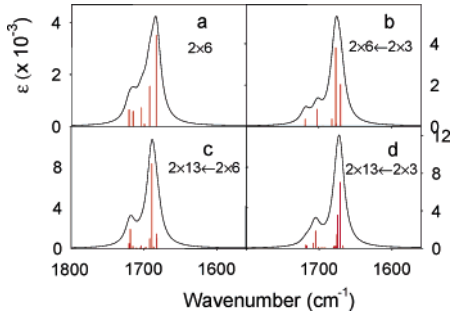

Figure 2. Simulated amide I′ IR spectra at the BPW91/6-31G** level, all N-deuterated, for the model structures of (a) 2 × 6 β-sheet DFT result; (b) 2 × 6 β-sheet transferred from 2 × 3 DFT; (c) 2 × 13 β-sheet transferred from 2 × 6 DFT; and (d) 2 × 13 β-sheet transferred from 2 × 3 DFT.

encompassing the two types of hydrogen-bonded rings found in an antiparallel β-structures. These models cannot encompass longer-range intrastrand coupling at the ab initio level, although it could be estimated by TDC methods.[70] For a single extended β-strand of eight residues, we showed that the amide I (and II) IR spectra resulting either from a fully ab initio calculation or by transfer of parameters from a triamide strand were effectively identical when simulated with realistic band shapes.[71]

To determine if this apparently local dominance of interactions held with the addition of longer range cross-strand coupling, we have now computed DFT spectral parameters for two hexaamide strands, (Ac-Ala$_5$-NHCH$_3$)$_2$, here termed 2 × 6, constrained to an antiparallel conformation (Figure 1c). The comparison of the amide I IR spectra obtained by this full ab initio 2 × 6 calculation, with that obtained by a transfer (symbolized as 2 × 6 ← 2 × 3) onto that same structure from the shorter original calculation, 2 × 3 or (Ac-Ala$_2$-NHCH$_3$)$_2$ (Figure 1a), are shown in the upper part of Figure 2 as cases a and b, respectively. After convolution with realistic line widths, the ab initio-determined intensity envelopes are qualitatively similar except that the ab initio 2 × 6 result has higher frequencies, thus 2 × 6 ← 2 × 3 results in a main amide I feature ∼20 cm^{-1} lower than 2 × 6, with an apparent increase in dispersion of modes. This suggests that the critical couplings are represented in the 2 × 3 model, even though other forces result in some frequency shift from the 2 × 6 result.

In the bottom part of Figure 2, the results of transferring the 2 × 3 and the 2 × 6 parameters to a longer β-sheet model (Figure 1d), with 13 amides in each strand, yield the cases shown in Figure 2c, 2 × 13 ← 2 × 6, and Figure 2d, 2 × 13 ← 2 × 3, respectively. The average frequencies for the 2 × 13 ← 2 × 6-based calculation are again higher by almost 20 cm^{-1} as compared to the 2 × 13 ← 2 × 3-based result, since the frequencies reflect the FF, but the band shapes are nearly identical, reflecting the couplings. The most intense maximum is separated from the higher frequency maximum by ∼30 cm^{-1} in each 2 × 13 model. The basic β-like intensity distribution pattern is maintained in each calculation with the bulk of the intensity in one or two low-frequency modes corresponding to out-of-phase motion of C═O groups on sequential residues. Beyond the amide I′, the other modes such as amide II′ and amide III′ are very similar between the two FF. Thus, other than amide I average frequency, the length of the fragment used to obtain parameters for transfer had very little effect on the spectral shape of a longer polymer, suggesting local interactions are dominant.

To investigate the effect of computational level on these spectral simulations, the 2 × 3 antiparallel β-structure spectral

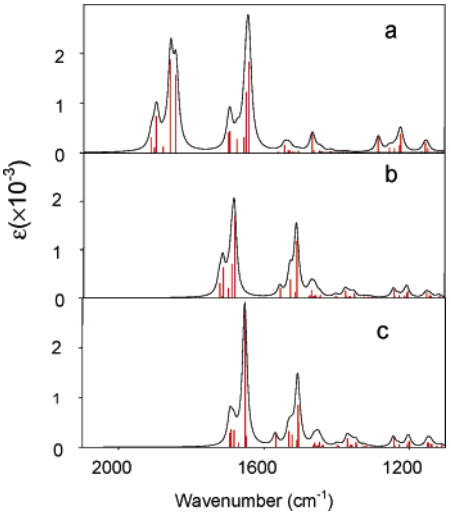

Figure 3. Simulated IR spectra for the amide I, II, and III regions for the ab initio computed 2 × 3 N−H-containing β-sheet (nondeuterated), at the (a) HF/6-31G**, (b) BPW91/6-31G**, and (c) BPW91/6-31++G** levels.

parameters were computed at the HF/6-31G**, BPW91/6-3IG*, BPW91/6-31G**, and BPW91/6-31++G** levels. The results for natural (nondeuterated) isotopic composition are compared in Figure 3 for the wider region of frequencies containing the amide I, II, and III vibrations. The unrealistically high amide I frequencies obtained at the HF level (Figure 3a) are partially corrected in the DFT calculations, which results in a large frequency shift (down), as is known and was expected from earlier work.[28,72−75] An increase in polarization from 6-31G* (comparison not shown) to 6-31G** with the BPW91 functional had very little impact on the spectra in this region, for example, it caused minor changes in separation of the in-phase and out-of-phase amide modes. However, adding diffuse functions, i.e., 6-31++G** (Figure 3c), does have a significant impact, lowering the amide I frequencies to a range close to that which is observed experimentally yet leaving the amide II and III about the same. We also suppose that the diffuse functions (represented by ++) describe the hydrogen bonding better. Their effect is consistent with our previous study dealing with the impact of altered basis sets that include more diffuse polarization functions.[76] Apart from this frequency shift and further concentration of amide I intensity into one mode, thereby enhancing its intensity, the spectral shape obtained with the biggest basis remains similar. Obviously, calculation with the diffuse atomic orbitals results in a much higher computer cost. Our experience was, that for the 2 × 3 peptide, computation of the harmonic vibrational frequencies with an Intel Xeon 2.8 GHz processor took 426 h with the 6-311++G** basis (774 functions), as opposed to 14 h for the 6-31G** basis (620 functions).

The effect of an aqueous environment on the spectra is important, and this points to a potential weakness of these methods, which are essentially vacuum calculations. Including solvent molecules places a large computational burden on the simulations, limiting the size of the system one can consider directly. We have shown with model calculations on *N*-methylacetamide (NMA)[76] that include explicit or implicit (in this case the COSMO-polarized continuum model)[55] solvent that the amide I transition shifts down in frequency from the vacuum result but is still high unless both are used. The same is qualitatively true of longer (helical) extended peptides with explicit waters of solvation.[56] For helical peptides, the relative distribution of intensity is maintained between vacuum and solvent-containing calculations, implying that the interresidue

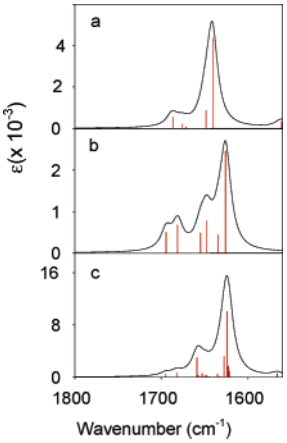

Figure 4. Simulated IR spectra for (a) 2 × 3 peptide with the COSMO model and (b) 2 × 3·12D_2O peptide, which includes 12 explicit water (D_2O) molecules. (c) Result of subsequent transfer of 2 × 3·12D_2O parameters onto the model 2 × 13·D_2O β-sheet with explicit waters, all proton-exchanged, i.e., D_2O and N-deuterated.

coupling is not distorted by solvent. This is perhaps not surprising, since in α-helices most of the C═O groups are already H-bonded. For 3_1 helices the impact of solvent is bigger since none of the C═Os are H-bonded in a vacuum. Incorporating solvent in a simulation for a β-sheet conformation has both effects: the C═O groups that point away from the other strand, and thus are not H-bonded in a vacuum, will change character on solvation, becoming fully H-bonded, while the inner ones change much less. This suggests that β-sheet contributions (diagonal force constant) to the relative frequency shifts will not be the same for these two types of residues and relative changes can occur.

To find out how the solvent perturbs the coupling patterns in present models, we have computed spectra for the 2 × 3 peptide with the same DFT level but including a COSMO correction, as shown in Figure 4a. We have additionally computed force field and intensity parameters for this molecule with 12 waters of hydration included, which make up the full first layer of inner hydrogen-bonded water, two per external directed amide C═O, and one per external N−H and internal C═O (Figure 1b). Due to the pucker of the sheet, these internal C═O−H-bonded waters are all on one side of the sheet and correspond to hydration patterns found in X-ray studies of similar protein structures.[77] The amide I′ frequencies obtained for this 2 × 3·12D_2O system (Figure 4b) now effectively match the expected experimental frequency range for short, double-stranded β-sheets having an intense low-frequency feature (arising predominantly from one out-of-phase mode) at ∼1625 cm^{-1} and a weaker high-frequency band at ∼1660 cm^{-1}. After transfer of these parameters to the 2 × 13 model with explicit waters (Figure 1e), the amide I dispersion appears reduced, much as computed for the vacuum 2 × 13 case, since the highest frequency amide I modes, which involve terminal group motions, have little relative intensity (Figure 4c). However, the actual dispersion of modes is the same as for the 2 × 3·12D_2O.

Isotopic Substitution Patterns. For the two-stranded six-amide model antiparallel sheet, the spectral consequences of placing ^{13}C labels on various positions in the strands were investigated more systematically. In Figure 5, absorption spectra for different substitution patterns are simulated for ^{13}C labeling on the 2 × 6 model dimer. For the substitutions presented in Figure 5 and Table 2, an arbitrary numbering of the carbonyl carbon atoms is used, starting at the N-terminus of the peptide chain, according to Chart 1.

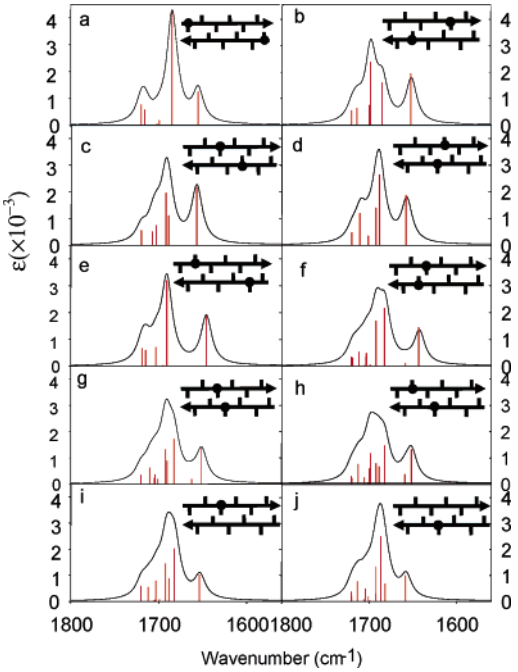

Figure 5. Amide I absorption pattern for the 2 × 6 model β-sheet with different ^{13}C isotopic substitutions, as calculated at the BPW91/6-31G** level. (a−c) Cross-strand H-bonded C═O residues, with the same position in each strand, where (c) forms a large, 14-atom ring; (d, e, h) outer-directed C═O groups; (f) small, 10-atom H-bond ring inner-directed C═O; (g, h) close-lying coupling of in- and out-pointing C═O; (i, j) single labels.

Experimentally, antiparallel pairs with both strands labeled on the same positions are the simplest result of forming a β-sheet from nonbonded strands. For such a structure, the labeled C═O groups would be well-separated from each other unless they occurred in the center of the strand. The spectra with the peptide labeled on the same position in each strand but toward the ends (Figure 5a,b) are similar to what is obtained for just a single strand being labeled on an H-bonded C═O (Figure 5i), since long-range coupling is very weak. When the labels are in the central positions, where cross-strand coupling becomes important, the pattern changes more (Figure 5c).

Due to the even number of residues in our model oligopeptide, 2 × 6, and its C_2 symmetry, substituting the center positions makes the labeled residues form a large (14 atoms) H-bonded ring. All the ^{13}C═O IR intensity in this case is in the higher frequency out-of-phase component, which is split about 6 cm^{-1} from its symmetric (in-phase) partner. The low intensity for the in-phase ^{13}C═O coupling makes sense here since the local transition dipoles cancel each other due to lying close to the plane and having C_2 symmetry. If the center H-bonded ring were the alternate smaller (10-atom) type, the coupling would have been stronger, ∼15 cm^{-1} in our example (Figure 5f), and the lower frequency component would be the more intense (in this 2 × 6 model peptide, small rings must be simulated by choosing a nonnatural labeling pattern). This reversal of coupling makes the large and small ring structures differ in their apparent ^{13}C peak frequency by ∼10 cm^{-1}, which is in excellent agreement with our results for labeled β-hairpins.[48] From the computed splitting of the ^{13}C═O modes, $\Delta\omega = 2V$, the coupling constant between the labeled positions can be estimated for use in the coupled oscillator approximation or for comparison with the coupling constants that would result by fitting data from various experimental sources or from computing the TDC that would result from the structures used.

TABLE 2: Comparison of the DC and ab Initio Models for the $^{13}C{=}O$ Stretching Interaction

		$\Delta\omega^a$ (cm^{-1})			D^b (debye^2)		
label position (^{13}C pattern)^c	d^d (Å)	ab initio 2×6	ab initio $2 \times 6 \leftarrow 2 \times 3$	TDC	ab initio 2×6	ab initio $2 \times 6 \leftarrow 2 \times 3$	TDC
a (1−7)	18.59	0.11	0.18	0.17	0.16/0.00	0.12/0.05	0.23/0.00
b (5−11)	12.78	0.01	0.63	0.24	0.22/0.00	0.26/0.00	0.23/0.00
c (3−9)	5.81	6.0	8.2	2.9	0.27/0.00	0.27/0.00	0.23/0.00
d (4−10)	6.66	−1.2	−1.4	−2.4	0.00/0.21	0.01/0.23	0.00/0.22
e (2−8)	10.45	1.32	0.59	0.34	0.24/0.00	0.23/0.00	0.23/0.00
f (3−11)	4.79	−15.3	−7.5	−18.6	0.01/0.16	0.00/0.18	0.00/0.23
g (3−10)	5.08	−11.3	−17.5	−15.7	0.02/0.16	0.06/0.13	0.02/0.20
h (2−10)	7.46	−7.4	−5.7	−4.71	0.04/0.15	0.00/0.20	0.00/0.22

[a] Difference between the frequency of the more and less intense IR bands. [b] Dipolar strengths for the higher/lower frequency bands. [c] Letters indicate the label position as shown in Figure 5; numbers in parentheses indicate positions of the labeled $^{13}C{=}O$, as in Chart 1. [d] Distance between the carbonyl carbon atoms.

CHART 1: Numbering of the Carbonyl Carbon Atoms in the 2 × 6 Dimer, from N to C Terminus

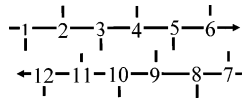

When a parallel set of computations is done for the same peptide structure but with a force field transferred from the 2 × 3 triamide, $(Ac\text{-}Ala_2\text{-}NHCH_3)_2$, the same patterns resulted with the exception of the quantitative values for the splittings. With a 2 × 3 transferred FF, the apparent coupling constants were actually comparable for the large and small ring constructions (see Table 2). This may arise from the fact that the small molecule, 2 × 3, though including an example of large and small rings, has them both on ends, including terminal residues. In the 2 × 6 molecule, there are three large rings, two on both ends and one in the middle. The terminal ring splitting is larger, 9.9 cm^{-1}, than for the center ring, 6 cm^{-1}. This end value is very close to what is obtained for the same ring in the 2 × 6 ← 2 × 3 case (9.4 cm^{-1}). This same sort of test is not possible for the small ring, but the pattern supports end effects as being important and provides a further rationale for our use of a 2 × 6 model for the coupling constant estimation. These coupling constants are thus more sensitive than the overall band envelope to the size of the fragment oligopeptide used for transfer, and these results expressly argue against attempting to use such simplified models for determining interstrand coupling interactions to a high degree of precision. The sign and order of magnitude are correct with the short peptides, but finer detail requires longer peptide models.

Taking a different point of view, if we go even further from a "natural" alignment of labels and just ask what happens if two labels have different relative positions in two H-bonded strands, we can simulate outer and inner labels which couple to create strong dipolar transitions (Figure 5g,h). Here if two labels are lined up, the splitting is as strong as for a small ring (11.3 cm^{-1}), and if offset by one residue, the splitting is about half that value (7.4 cm^{-1}). All of this supports proximity and dipole coupling as being important factors in the overall interstrand coupling. This importance of dipole coupling is presumably why such dipole-based calculations have succeeded in the past. However, when modes involving adjacent (or nearly so) bonds are coupled, the dipole approximation will be inadequate.[28,70,72] In Table 2 are listed values for the dipole-coupling-induced splitting computed with the geometrical relationships given by the 2 × 6 structures for the labeled C═O groups (see Calculations). The consistency of coupling constants for the 2 × 6 and 2 × 6 ← 2 × 3 results is clear and is quantitatively better than for the TDC results. However, the TDC does have the right qualitative variation.

Multiply Labeled Strands. As shown experimentally[20] and in our previous theoretical study,[10] use of two labels on a single strand of a multistranded sheet leads to decidedly different intensity patterns if the labeled residues are sequential or alternate in the peptide chain.[20] Another situation where such alternate labeling can occur is in monomer forms, when the sequence folds back on itself to form a hairpin. In this case we have explored various patterns of labeling and found, consistent with the above 2 × 6 model results, that those labeled C═O groups that are closest together couple the strongest, even across strands. The formation of a small H-bonded ring with two labeled C═O groups results in the largest shift (and lowest absolute frequency) of the ^{13}C band from the ^{12}C maximum, as shown in the results in Figure 5f and Table 2. This is particularly striking as compared to the larger ring in Figure 5c for the ab initio hexaamide result.

This pattern is preserved when the 2 × 6 FF is transferred to the 2 × 13 β-structure as shown in Figure 6a,b. The ^{13}C maximum for the small ring being lower in frequency than for the large ring is due to the stronger coupling causing a larger splitting between the ^{13}C modes combined with their lower energy component having the bulk of the dipole intensity. This pattern is consistent with various placements along the strands, giving a coupling resulting in $\Delta\omega \sim 11-15$ cm^{-1} for four different small rings (interior-pointing C═O groups) that were computed. For the larger ring the splitting is less, but in this case the higher frequency component is the more intense, which results in the large apparent shift of the observed ^{13}C band, as noted above and shown in Figure 6 and as we have seen experimentally.[48] This pattern persists for most positions in the sequence for these larger H-bonded rings, giving $\Delta\omega \sim 5$ cm^{-1}, with the exception of a ring formed with the end groups, which has an enhanced coupling, giving $\Delta\omega \sim 9$ cm^{-1}, as noted above. We have tested this characteristic here for our 2 × 13 models, but it holds just as well for a somewhat twisted hairpin with a type I′ β-turn (structure taken from intestinal fatty acid binding protein, PDB 1IFC).[48] Thus the frequency shift can be viewed as characteristic of the size (or type) of internal H-bonded ring formed and can be used to determine the alignment of strands. For a hairpin structure, this sort of pattern can also imply the generic type of turn that is formed, since the label positions are known from the synthesis design. The relative $^{13}C-^{12}C$ intensity is diagnostic as well, since the smaller ring has less intensity, though its ^{13}C band is shifted more. The larger ring, by contrast, with its smaller separation for the intense component, appears to borrow intensity from the ^{12}C modes and get enhanced, much as in the case of the alternate $^{13}C{=}O$ labeling discussed

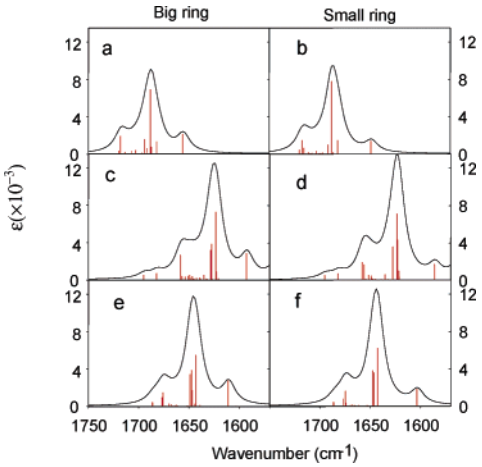

Figure 6. Comparison of shifts for two ^{13}C labels forming (a) large and (b) small H-bonded rings in the 2 × 13 ← 2 × 6 BPW91/6-31G** calculations, and the analogous (c, e) large- and (d, f) small-ring situation for the 2 × 13 ← 2 × 3 transfer based on (c, d) the explicit water model and (e, f) the BPW91/6-31++G** approximation. In each case the intensity of the in-phase ^{13}C═O mode is too weak to appear in the figure.

previously.[48] The key to this enhancement is coupling local modes to the alternately out-of-phase modes in each strand and coupling labeled C═Os across H-bonded strands so that the dipoles constructively interfere.

Carrying this further, comparison of transfer of parameters obtained from the 2 × 6 calculation (Figure 6a,b) with those from the 2 × 3 with diffuse functions (Figure 6e,f) or the 2 × 3·12D_2O (including a shell of waters) onto 2 × 13 (or 2 × 13·H_2O) structures (Figure 6c,d), shows qualitatively consistent patterns for the isotopic modes, both large and small ring. The relative frequency shift of the intense ^{13}C band from the ^{12}C peak is characteristic of the H-bond ring formed in each method. The 2 × 3 model with no water (not shown) does seem to have a slightly larger relative frequency shift for the ^{13}C modes, and due to the end effects discussed above for the 2 × 6 ← 2 × 3 calculation, the coupling for labeled ^{13}C═O in large and small rings with a 2 × 3 source is more alike than for the 2 × 6 source. The ^{13}C mode for the simulation with added water actually occurs below 1600 cm^{-1}, in qualitative agreement with experimental results.[48] These features in the explicit water calculation are distorted, see Figure 6c,d, but the coupling patterns are much like those seen in the 2 × 13 ← 2 × 3 calculations, the end effects making the coupling for large and small rings comparable, all yielding $\Delta\omega \sim 7-10$ cm^{-1}. However, the large ring still has its out-of phase mode higher in frequency, while for the small ring, the out-of-phase mode is lower in frequency and more intense, which leads to the small ring intensity maximum having a larger frequency separation from the dominant ^{12}C modes, but less intensity than the large ring, as seen in all the cases.

The alternate way of compensating for the solvent is use of the COSMO correction for water dipole effect or inclusion of more diffuse basis functions to improve the H-bond description and presumably lengthen the C═O bond. The frequency is known to correlate to the C═O bond length in amides.[76,78−80] The effect of the 6-31++G** basis set on the 2 × 13 ← 2 × 3 transfer is shown in Figure 6e,f. Again, since it is a 2 × 3-based transfer, the large and small ring coupling constants are roughly equal, with $\Delta\omega \sim 8$ cm^{-1}, out-of-phase to higher frequency, and $\Delta\omega \sim 7$ cm^{-1}, opposite sign splitting, respectively. Thus the pattern, large vs small ring relative intensity and shift, is not affected by basis set, core frequency, or water addition.

Effect of Twist. Real hairpins and most sheets are twisted in a right-handed sense. To simulate the effect of this variation, we incorporated isotope substitution in our previously reported variably twisted β-sheet models (as shown for the extremes of α, the twist angle, in Figure 7).[56] For the small ring formation (center of the strands), although the spectra shift in frequency, the splittings are almost impervious to twist, giving a ^{12}C maximum at 1668−79 cm^{-1} and a ^{13}C peak at 1628−30 cm^{-1} as the angle between end C═O groups is varied from $\alpha = 140°$ to −140°. For the large labeled ring simulation, the ^{13}C peak frequencies and intensities are higher, ranging from 1636 to 42 cm^{-1} with a similar shift of the main ^{12}C, but these calculations have added disruption of the ^{12}C modes since the symmetry is disturbed to make a big ring. These results show that the concept of large and small ring cross-strand coupling is maintained, with the intense ^{13}C component of the small ring being the lower one of the coupled pair. For the large ring, the intense coupled component is the higher frequency one (making the ^{13}C mode seem less shifted from the ^{12}C and more intense than the small ring). Thus, even with twisting, the lower frequency and lower intensity ^{13}C isotope shifted band indicates small ring formation. While an effect of twist is seen on the frequencies, it is modest, and, in both cases, the ^{13}C and ^{12}C frequencies steadily and smoothly increase as the twist angle α gets more negative, which indicates that this frequency dependence must be an overall force field effect and is not isotope-specific.

Discussion

These results show that the length and basis set are minor perturbations on the basic amide spectral band shapes obtained in a DFT-based simulation utilizing transfer of parameters from smaller to larger peptide of the same secondary structure. Molecular size used for the DFT calculation and the ability to model internal vs terminal interstrand coupling may affect the coupling constants between labeled sites more. None of these, including solvation, has much impact on the band shape observed, if one can correct for, or ignore, the basic frequency error (always too high for C═O), which is a property of the vacuum, ab initio calculations. In other words, if one seeks explanation of *observable* splittings and band shapes, vacuum DFT is sufficient. If one wants absolute frequencies, a correction is needed, and if one wants more precise couplings, longer peptide models are needed to avoid end effects. Clearly, including water or a solvent correction improves the frequencies computed in comparison to the experimental results for model β-sheet systems. Other research groups have shown this and have correlated the shift to solvent electric field or bond length effects at the C═O, which has been developed to an empirical FF correction.[78,79] For our uncorrected DFT calculations, some patterns have emerged around these computed amide I′ frequencies.

For the unlabeled molecule, a typical β-sheet pattern arises,[10] with a lower-intensity higher-frequency shoulder (in a vacuum calculated at ∼1720 cm^{-1}) corresponding to the outer C═O group vibrations and in-phase modes, and a stronger signal, with a maximum in a vacuum at 1683 cm^{-1}, originating from out-of-phase coupling (between strands) of those (alternate in a strand) C═O groups that form hydrogen bonds between the two peptide chains. Labeling of one C═O group pointing inside the sheet, thus H-bonded, results in a ^{13}C═O mode computed at 1645−1654 cm^{-1}, separated from the most intense ^{12}C maximum by 30−35 cm^{-1}. The unlabeled group absorbance is also

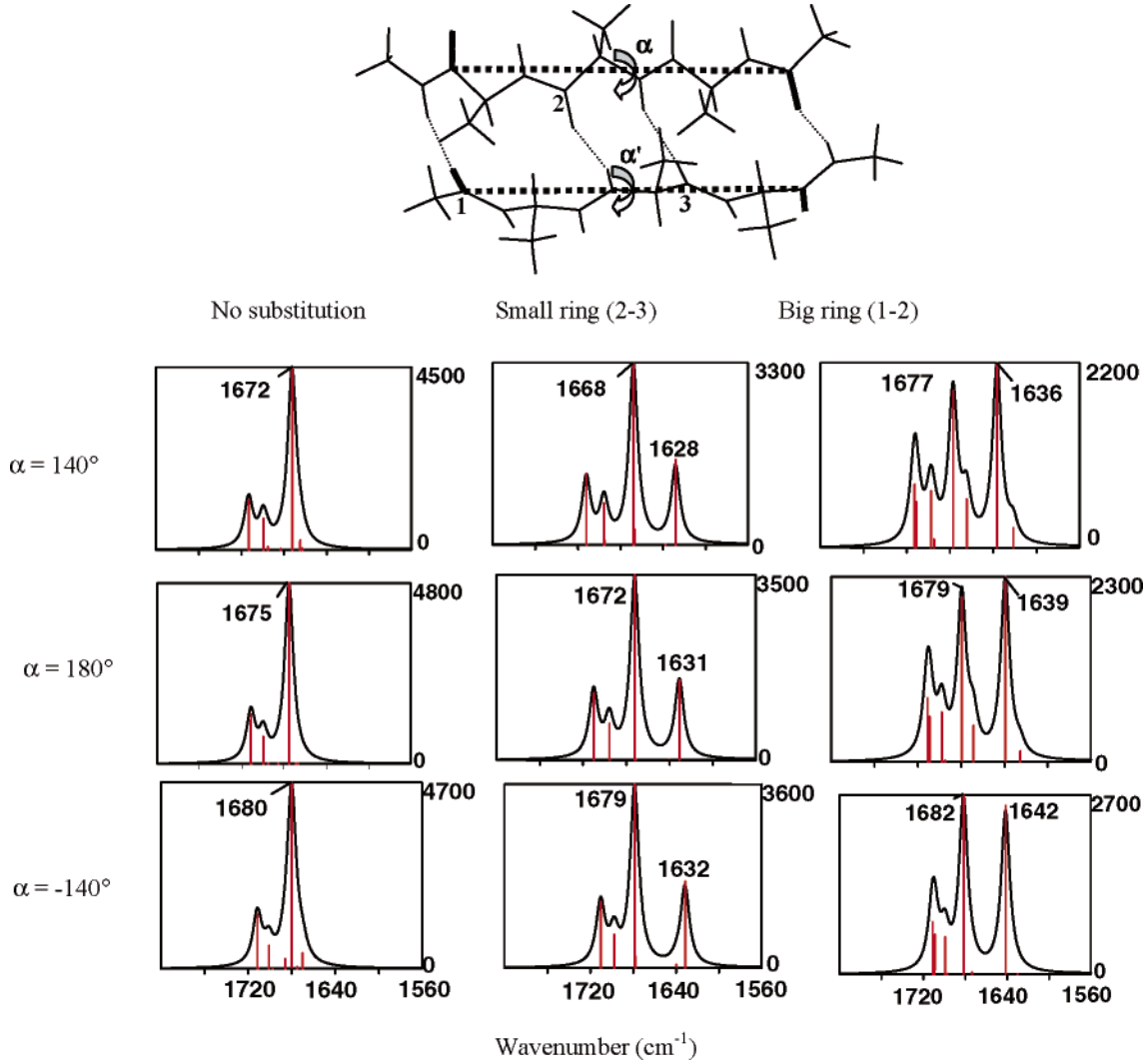

Figure 7. Absorption spectra: dependence of the amide I′ band ^{13}C isotopic effect on the β-sheet twist angle for 2 × 4 tetraamide model.[56] The twist (angle α) is defined as the torsional angle for the terminal C═O groups. Substitution sites are indicated in the sketch above the spectra but form a small ring between the center residues (there numbered 2−3) or a big ring on the end (1−2). C_2 symmetry (α = α′) and the BPW91/6-31G** level DFT method were used for the calculation.

perturbed by the labeling, so that the ^{12}C peak frequency shifts to higher wavenumbers (computed at ∼1691 cm^{-1}), magnifying the apparent isotope effect in the spectrum. This is due to disturbance of in-strand coupling by the ^{13}C, leaving a discontinuity in the ^{12}C═O exciton band.

This separation is amplified when another label is present in the other strand, due to interstrand coupling. Here, the coupling between the two ^{13}C═O groups in a small (10-atom) H-bond ring can cause the two modes to split by 15 cm^{-1} and build up intensity in the lower-frequency out-of-phase component computed at 1643 cm^{-1}. For the larger H-bond ring (14 atom), not only is the splitting smaller (6 cm^{-1}) but also the intensity builds up in the higher-frequency component computed at 1657 cm^{-1}. Thus these can be thought of as constructive and destructive cases with respect to ^{13}C labeling, amplifying and damping the isotopic frequency shift, respectively, but having the opposite effect in terms of intensities. Both patterns can be used to identify β-sheet formation (according to the up- and down-frequency shift as compared to the effect of a single label). While experimentally the larger shift in the small ring is more convenient to identify, in some cases the higher intensity in the larger ring will be important (especially for relatively dilute labels).

Similar behavior can be observed for the substitution of the carboxyl groups pointing to the outside of the two strands. A single substitution (case j in Figure 5) gives a rise to a band computed at 1658 cm^{-1}, which is higher than the above values due to not being H-bonded and which can be further amplified by a constructive (in-phase, in this case) coupling of two chromophores. Coupling two labels causes a split of 11 cm^{-1} with the lower-wavenumber component shifting to 1651 cm^{-1}. Outer- vs inner-carbonyl labeling is seemingly arbitrary for an experimental situation with single strands aggregating, since the option will depend on alignment of the strands and the real frequencies will be affected by solvent shifts, so discrimination will be difficult. For multiple strands these will be effectively equivalent concepts. If one can select for labels on the inner pointing groups, the apparent isotopic shift will be larger and the coupling stronger, leading to larger splitting and enhancing detection.

Such control is possible in hairpin model systems where the turn residues are selected by design and the inner- and outer-pointing C═O groups become separable. We have shown that the computed patterns in such hairpins match those demonstrated in these dimer strand computations, in other words, that the turns do not perturb them significantly, and we have shown they also fit observed isotope shifts and intensity distributions in model labeled hairpin molecules.[48] The shift pattern for the ^{13}C band in designed hairpins is consistent with those in Figure 6, with

the spectra of labels in the large ring being less shifted and more intense and those in the small ring being better separated and less intense, and is relatively independent of position in the strands.

The intensity patterns observed for these isotope coupling models can be easily explained by visualization of the normal mode coordinates. For example, in the case of labeled C═O groups in the small ring, if both the C═O groups become shorter or longer at the same time, this in-phase mode has cancellation of the two transition dipole moments, leaving a weak residual dipole. For out-of-phase coupling the dipole moments add up, leading to a large net dipole and enhancement in the absorption spectrum. The same pattern can be observed in the large ring, except that the sign of the coupling constant is reversed so that the intense out-of-phase mode shifts up in frequency, not down, from the isolated ^{13}C label position.

Longer, Twisted, and Hydrated β-Sheets. We have used a 13-amide β-sheet dimer as a computational model to study effects of the computational level, hydration, and length effects after transfer from a smaller DFT calculation to a larger uniform system. The geometries of the vacuum and hydrated peptide can be seen in Figure 1; its force field and dipole derivative tensors were transferred from computations on smaller segments both vacuum and solvent-corrected. The typical amide I β-sheet profile is conserved for all the models, but hydration causes a significant shift of the absorption frequencies toward experimental values. The diffuse-function-containing basis set (6-31++G**) for the 2 × 3 vacuum model leads to lower frequencies and a better agreement with experiment than the smaller polarized basis sets (6-31G**). Diffuse functions better model H-bonding effects, which are important for interstrand coupling that is here tested by isotopic labeling. Somewhat surprisingly, the longer 2 × 6 amide leads to a minor shift up in frequency for the band maximum.

The effect of placing the large or small ring on the terminal segments of the peptide was also investigated. Clearly, in both cases placing the ring at the end causes a relatively minor perturbation to the absorption profile, which suggests that use of such labeling to detect experimental β-sheet formation has wider potential. The large ring is affected more than the small one.

The effect of the basis set on the large and small ring isotope spectral patterns was explored. Apparently, except for the frequency shift following the pattern found earlier, the patterns are consistent; namely, the constructive and destructive couplings for the small and large ring cases are conserved.

Finally, the effect of β-sheet twist on the coupling pattern was simulated with a 2 × 4 amide peptide with a series of twist geometries that had been previously optimized at the BPW91/6-31G** level.[56] The twist does not significantly influence absorption spectra of the nonsubstituted peptide and also does not disturb the coupling. For both the large and small ring patterns, variation from positive to negative values of overall twist causes a minor increase of the ^{13}C band absorption (~10%) and the frequency (4−6 cm^{-1}) but no change in the splitting.

Parallel sheet segments and differentiation of antiparallel and parallel sheets were explicitly not addressed in this paper. Previous work has shown these unlabeled structures can yield differentiable IR patterns, if both form flat extended sheets.[71] However, when such sheets are twisted, differentiation becomes difficult. Perhaps with labeling, the coupling would be a means of more positive differentiation. The design of comparable experiments to test such labeling predictions is difficult, since parallel hairpins (where one can control of strand content and oligomerization) must be prepared by use of turn mimetics. Alternatively, parallel β-sheets can be obtained in proteins or as multistranded structures, which will be addressed in a forthcoming paper.

TDC Model. For several double isotopic substitutions, the ab initio values of the frequency split of the two ^{13}C═Os and their dipole strengths are compared to those obtained from the coupled oscillator or TDC model in Table 2. It is apparent that the sense of frequency splitting obtained by this semiempirical method follows the ab initio relative ordering, although the absolute values obtained differ by up to ~100%. Also, the relative IR intensities (dipole strengths) of the two components obtained by the TDC model are quite reasonable. This can be explained by the relatively weak dipolar interaction between the C═O chromophores, resulting from their large separation (>5 Å) and the indirect nature of their connection via covalent bonds. Thus much, but not nearly all, of the coupling interaction arises from the dipole−dipole term on which the model is based. Obviously, the model itself cannot describe finer intensity variations (since the sum of the dipole strengths for the higher and lower frequency bands must be constant) and is dependent on arbitrary parameters. Thus, since the TDC model has the correct sense, if the couplings are parametrized, good simulations of the ^{13}C mode patterns can yield qualitatively useful results, as has been seen by others.[20,53,81] However, our ab initio results show this dipolar interaction is only part of the picture and that it leaves out the interaction, though higher order, with the ^{12}C modes. Thus more subtle discriminations of intensity patterns demand quantum mechanically based modeling.

Conclusions

We have demonstrated that the ^{13}C coupling across antiparallel β-sheet strands can be identified in the absorption spectrum. The small ring coupling appears most convenient for an experimental identification of β-sheet formation, giving the biggest frequency shift from the ^{12}C bands, but larger ring coupling yields intensity enhancement that can be the basis of an alternate detection scheme. These patterns appear to be an inherent property of the sheet structure, undisturbed by the hydration and a modest β-sheet twist.

Acknowledgment. This work was supported by grants (to P.B.) from the Grant Agency of the Academy of Sciences (A4055104) and the Grant Agency of the Czech Republic (Grant 203/01/0031), by a grant (to T.A.K.) from the National Science Foundation (CHE03-16014), and in part by a grant from the donors of the Petroleum Research Fund, administered by the American Chemical Society. We thank Dr. Jan Kubelka for discussions of β-sheet structures and for carrying out preliminary computations and Mrs. Rong Huang for assistance with figures and analyses of isotope patterns.

References and Notes

(1) Mantsch, H. H.; Chapman, D. *Infrared Spectroscopy of Biomolecules*; Wiley-Liss: Chichester, U.K., 1996.

(2) Haris, P. I.; Chapman, D. *Biopolymers* **1995**, *37*, 251−263.

(3) Byler, D. M.; Susi, H. *Biopolymers* **1986**, *25*, 469−487.

(4) Williams, R. W.; Dunker, A. K. *J. Mol. Biol.* **1981**, *152*, 783−813.

(5) Tadesse, L.; Nazarbaghi, R.; Walters, L. *J. Am. Chem. Soc.* **1991**, *113*, 7036−7037.

(6) Fabian, H.; Chapman, D.; Mantsch, H. H. In *Infrared Spectroscopy of Biomolecules*; Mantsch, H. H., Chapman, D., Eds.; Wiley-Liss: Chichester, U.K., 1996; pp 341−352.

(7) Decatur, S. M.; Antonic, J. *J. Am. Chem. Soc.* **1999**, *121*, 11914−11915.

(8) Halverson, K.; Sucholeiki, I.; Ashburn, T. T.; Lansbury, R. T. *J. Am. Chem. Soc.* **1991**, *113*, 6701−6703.
(9) Silva, R. A. G. D.; Kubelka, J.; Decatur, S. M.; Bouř, P.; Keiderling, T. A. *Proc. Natl. Acad. Sci. U.S.A.* **2000**, *97*, 8318−8323.
(10) Kubelka, J.; Keiderling, T. A. *J. Am. Chem. Soc.* **2001**, *123*, 6142−6150.
(11) Gordon, L. M.; Lee, K. Y. C.; Lipp, M. M.; Zasadzinski, J. A.; Walther, F. J.; Sherman, M. A.; Waring, A. J. *J. Peptide Res.* **2000**, *55*, 330−347.
(12) Decatur, S. M. *Biopolymers* **2000**, *54*, 180−185.
(13) Barber-Armstrong, W.; Donaldson, T.; Wijesooriya, H.; Silva, R. A. G. D.; Decatur, S. M. *J. Am. Chem. Soc.* **2004**, *126*, 2339−2345.
(14) Huang, R.; Kubelka, J.; Barber-Armstrong, W.; Silva, R. A. G. D.; Decatur, S. M.; Keiderling, T. A. *J. Am. Chem. Soc.* **2004**, *126*, 2346−2354.
(15) Huang, C. Y.; Getahun, Z.; Zhu, Y.; Klemke, J. W.; DeGrado, W. F.; Gai, F. *Proc. Natl. Acad. Sci. U.S.A.* **2002**, *99*, 2788−2793.
(16) Huang, C. Y.; Getahun, Z.; Wang, T.; DeGrado, W. F.; Gai, F. *J. Am. Chem. Soc.* **2001**, *123*, 12111−12112.
(17) Venyaminov, S. Y.; Hedstrom, J. F.; Prendergast, F. G. *Proteins: Struct., Funct., Genet.* **2001**, *45*, 81−89.
(18) Silva, R. A. G. D.; Nguyen, J. Y.; Decatur, S. M. *Biochemistry* **2002**, *51*, 15296−15303.
(19) Silva, R. A. G. D.; Barber-Armstrong, W.; Decatur, S. M. *J. Am. Chem. Soc.* **2003**, *125*, 13674−13675.
(20) Brauner, J. W.; Dugan, C.; Mendelson, R. *J. Am. Chem. Soc.* **2000**, *122*, 677−683.
(21) Paul, C.; Wang, J. P.; Wimley, W. C.; Hochstrasser, R. M.; Axelsen, P. H. *J. Am. Chem. Soc.* **2004**, *126*, 5843−5850.
(22) Barany, G.; Merrifield, R. B. In *The Peptides, Vol. 2*; Gross, E., Meinhofer, J., Eds.; Academic Press: New York, 1980; Vol. 2, pp 1−284.
(23) Fang, C.; Wang, J.; Charnley, A. K.; Barber-Armstrong, W.; Smith, A. B., III; Decatur, S. M.; Hochstrasser, R. M. *Chem. Phys. Lett.* **2003**, *382*, 586−592.
(24) Torres, J.; Kukol, A.; Goodman, J. N.; Arkin, I. T. *Biopolymers* **2001**, *59*, 396−401.
(25) Zhang, M. J.; Fabian, H.; Mantsch, H. H.; Vogel, H. J. *Biochemistry* **1994**, *33*, 10883−10888.
(26) Paul, C.; Wang, J.; Wimley, W. C.; Hochstrasser, R. M.; Axelsen, P. H. *J. Am. Chem. Soc.* **2004**, *126*, 5843−5850.
(27) Harris, P. I.; Robillard, G. T.; van Dijk, A. A.; Chapman, D. *Biochemistry* **1992**, *31*, 6279−6284.
(28) Kubelka, J.; Silva, R. A. G. D.; Bouř, P.; Decatur, S. M.; Keiderling, T. A. In *Chirality: Physical Chemistry*; Hicks, J. M., Ed.; ACS Symposium Series, Vol. 810; American Chemical Society: Washington, DC, 2002; pp 50−64.
(29) Bouř, P.; Sopková, J.; Bednárová, L.; Maloň, P.; Keiderling, T. A. *J. Comput. Chem.* **1997**, *18*, 646−659.
(30) Bouř, P.; Kubelka, J.; Keiderling, T. A. *Biopolymers* **2000**, *53*, 380−395.
(31) Eker, F.; Cao, X.; Nafie, L.; Schweitzer-Stenner, R. *J. Am. Chem. Soc.* **2002**, *124*, 14330−14341.
(32) Schweitzer-Stenner, R.; Eker, F.; Huang, Q.; Griebenow, K. *J. Am. Chem. Soc.* **2001**, *123*, 9628−9633.
(33) Eker, F.; Cao, X. L.; Nafie, L.; Huang, Q.; Schweitzer-Stenner, R. *J. Phys. Chem. B* **2003**, *107*, 358−365.
(34) Hamm, P.; Lim, M.; Hochstrasser, R. M. *J. Phys. Chem.* **1998**, *102*, 6123−6138.
(35) Woutersen, S.; Hamm, P. *J. Phys.: Condens. Matter* **2002**, *14*, 1035−1062.
(36) Woutersen, S.; Hamm, P. *J. Chem. Phys.* **2001**, *114*, 2727−2737.
(37) Woutersen, S.; Hamm, P. *J. Phys. Chem. B* **2000**, *104*, 11316−11320.
(38) Fang, C.; Wang, J.; Kim, Y. S.; Charnley, A. K.; Barber-Armstrong, W.; Smith, A. B.; Decatur, S. M.; Hochstrasser, R. M. *J. Phys. Chem. B* **2004**, *108*, 10415−10427.
(39) Ge, N. H.; Zanni, M. T.; Hochstrasser, R. M. *J. Phys. Chem. A* **2002**, *106*, 962−972.
(40) Zanni, M. T.; Ge, N. H.; Kim, Y. S.; Hochstrasser, R. M. *Proc. Natl. Acad. Sci. U.S.A.* **2001**, *98*, 11265−11270.
(41) Ramirez-Alvarado, M.; Blanco, F.; Serrano, L. *Nat. Struct. Biol.* **1996**, *3*, 604−612.
(42) Ramirez-Alvarado, M.; Kortemme, T.; Blanco, F. J.; Serrano, L. *Bioorg. Med. Chem.* **1999**, *7*, 93−103.
(43) Gellman, S. H. *Curr. Opin. Struct. Biol.* **1992**, *2*, 717−725.
(44) Cochran, A. G.; Skelton, N. J.; Starovasnik, M. A. *Proc. Natl. Acad. Sci. U.S.A.* **2001**, *98*, 5578−5583.
(45) Hilario, J.; Kubelka, J.; Keiderling, T. A. *J. Am. Chem. Soc.* **2003**, *125*, 7562−7574.
(46) Hilario, J.; Kubelka, J.; Syud, F. A.; Gellman, S. H.; Keiderling, T. A. *Biopolymers* (*Biospectroscopy*) **2002**, *67*, 233−236.
(47) Setnička, V.; Hilario, J.; Keiderling, T. A. (submitted for publication).
(48) Setnička, V.; Huang, R.; Thomas, C. L.; Etienne, M. A.; Kubelka, J.; Hammer, R. P.; Keiderling, T. A. (submitted for publication).
(49) Krimm, S.; Abe, Y. *Proc. Natl. Acad. Sci. U.S.A.* **1972**, *69*, 2788−2792.
(50) Moore, W. H.; Krimm, S. *Proc. Natl. Acad. Sci. U.S.A.* **1975**, *72*, 4933−4935.
(51) Barron, L. D. *Molecular Light Scattering and Optical Activity*; Cambridge University Press: Cambridge, U.K., 1989.
(52) Bouř, P.; Keiderling, T. A. *J. Am. Chem. Soc.* **1992**, *114*, 9100−9105.
(53) Choi, J.; Ham, S.; Cho, M. *J. Chem. Phys.* **2002**, *117*, 6821−6832.
(54) Richardson, J. S.; Richardson, D. C. In *Prediction of Protein Structure and the Principles of Protein Conformation*; Fasman, G. D., Ed.; Plenum: New York, 1989; pp 1−98.
(55) Klamt, A.; Schuurmann, G. *J. Chem. Soc., Perkin Trans.* **1993**, *2*, 799−805.
(56) Bouř, P.; Keiderling, T. A. *J. Mol. Struct. (THEOCHEM)* **2004**, *675*, 95−105.
(57) Bouř, P.; Keiderling, T. A. *J. Chem. Phys.* **2002**, *117*, 4126−4132.
(58) Becke, A. D. In *Modern electronic structure theory*; Yarkony, D. R., Ed.; World Scientific: Singapore, 1995; Vol. 2, pp 1022−1046.
(59) Becke, A. *Phys. Rev. A* **1988**, *38*, 3098−3100.
(60) Bouř, P.; McCann, J.; Wieser, H. J. *Phys. Chem. A* **1998**, *102*, 102−110.
(61) Frisch, M. J.; Trucks, G. W.; Schlegel, H. B.; Scuseria, G. E.; Robb, M. A.; Cheeseman, J. R.; Zakrzewski, V. G.; Montgomery, J. A., Jr.; Stratmann, R. E.; Burant, J. C.; Dapprich, S.; Millam, J. M.; Daniels, A. D.; Kudin, K. N.; Strain, M. C.; Farkas, O.; Tomasi, J.; Barone, V.; Cossi, M.; Cammi, R.; Mennucci, B.; Pomelli, C.; Adamo, C.; Clifford, S.; Ochterski, J.; Petersson, G. A.; Ayala, P. Y.; Cui, Q.; Morokuma, K.; Malick, D. K.; Rabuck, A. D.; Raghavachari, K.; Foresman, J. B.; Cioslowski, J.; Ortiz, J. V.; Stefanov, B. B.; Liu, G.; Liashenko, A.; Piskorz, P.; Komaromi, I.; Gomperts, R.; Martin, R. L.; Fox, D. J.; Keith, T.; Al-Laham, M. A.; Peng, C. Y.; Nanayakkara, A.; Gonzalez, C.; Challacombe, M.; Gill, P. M. W.; Johnson, B.; Chen, W.; Wong, M. W.; Andres, J. L.; Gonzalez, C.; Head-Gordon, M.; Replogle, E. S.; Pople, J. A. Gaussian 98, Revision A.6; Gaussian, Inc.: Pittsburgh, PA, 1998.
(62) Choi, J. H.; Cho, M. *J. Chem. Phys.* **2004**, *120*, 4383−4392.
(63) Bouř, P. *Chem. Phys. Lett.* **2002**, *365*, 82−88.
(64) Chen, X. G.; Schweitzer-Stenner, R.; Krimm, S.; Mirkin, N. G.; Asher, S. A. *J. Am. Chem. Soc.* **1994**, *116*, 11141−11142.
(65) Holtzwarth, G.; Chabay, I. *J. Chem. Phys.* **1972**, *57*, 1632.
(66) Tinoco, I. *Radiat. Res.* **1963**, *20*, 133−139.
(67) Miyazawa, T. *J. Chem. Phys.* **1960**, *32*, 1647−1652.
(68) Torii, H.; Tasumi, M. *J. Chem. Phys.* **1992**, *96*, 3379−3387.
(69) Krimm, S.; Bandekar, J. *Adv. Protein Chem.* **1986**, *38*, 181−364.
(70) Kubelka, J. Ph.D. Thesis, University of Illinois, 2002.
(71) Kubelka, J.; Keiderling, T. A. *J. Am. Chem. Soc.* **2001**, *123*, 12048−12058.
(72) Bouř, P.; Keiderling, T. A. *J. Am. Chem. Soc.* **1993**, *115*, 9602−9607.
(73) Bouř, P.; Kubelka, J.; Keiderling, T. A. *Biopolymers* **2002**, *65*, 45−69.
(74) Abdali, S. J.; Jalkanen, K. J.; Cao, X.; Nafie, L. A.; Bohr, H. *Phys. Chem. Chem. Phys.* **2004**, *6*, 2434−2439.
(75) Frimand, K.; Bohr, H.; Jalkanen, K. J.; Suhai. S. *Chem. Phys.* **2000**, *255*, 165−194.
(76) Kubelka, J.; Keiderling, T. A. *J. Phys. Chem. A* **2001**, *105*, 10922−10928.
(77) Aravinda, S. H.; Harini, V. V.; Shamala, N.; Das, C.; Balaram, P. *Biochemistry* **2004**, *43*, 1832−1846.
(78) Ham, S.; Kim, J. H.; Lee, H.; Cho, M. *J. Chem. Phys.* **2003**, *118*, 3491−3498.
(79) Ham, S.; Cho, M. *J. Chem. Phys.* **2003**, *118*, 6915−6922.
(80) Bouř, P. J. Chem. Phys. **2003**, *119*, 11253−11262.
(81) Schweitzer-Stenner, R. *J. Phys. Chem. B* **2004**, *108*, 16965−16975.